The Effect of Solvent Dielectric Properties on the Collection of Oriented Electrospun Fibers

Zaicheng Sun,[1] Joseph M. Deitzel,[1] Jeff Knopf,[1] Xing Chen,[4] John W. Gillespie, Jr.[1,2,3]

[1]*Center for Composite Materials, University of Delaware, Newark, Delaware 19716*
[2]*Department of Material Science and Engineering, University of Delaware, Newark, Delaware 19716*
[3]*Department of Civil and Environmental Engineering, University of Delaware, Newark, Delaware 19716*
[4]*Department Of Physics and Astronomy, University of Delaware, Newark, Delaware 19716*

Received 30 June 2010; accepted 9 August 2011
DOI 10.1002/app.35454
Published online 29 January 2012 in Wiley Online Library (wileyonlinelibrary.com).

ABSTRACT: A simple approach to electrospinning has been developed that enables the collection of polymer, ceramic, and multiphase composite fibers, in quantity, with a high degree of spatial orientation. It has been demonstrated that a careful choice of solvent effectively eliminates the onset of the characteristic "bending" instability that is commonly associated with the electrospinning process. This allows collection of spatially oriented submicron electrospun fibers on a rotating drum without the need for elaborate mechanical or electrostatic manipulation of the electrospinning jet and/or collection target (Deitzel, J. M.; Kleinmeyer, J. D. et al. Polymer 2001, 42, 8163, Zussman, E.; Theron, A.; et al. Appl Phys Lett 2003, 82, 973, and Li, D. Wang, Y. L.; et al. Nano Lett 2003, 3, 1167). Fibers have been electrospun from a series of model polyethylene oxide/$CHCl_3$ solutions with a range of conductivities. The experimental data confirms theoretical predictions that the onset of the bending instability is a function of the available "free" charge in the solution, which in turn is strongly influenced by the dielectric constant of the solvent. The results show that fiber orientation becomes random as the conductivity increases, indicating the need for the surface charge density to exceed a critical threshold in order for the bending instability to initiate. This method has been experimentally demonstrated with other low-dielectric constant solvents and other common polymer, ceramic, and composite materials. Furthermore, it has been demonstrated that fibers electrospun from these solutions can be mechanically drawn to submicron dimensions ($\sim$ 200–500 nm) by controlling drum speed. © 2012 Wiley Periodicals, Inc. J Appl Polym Sci 125: 2585–2594, 2012

Key words: electrospinning; oriented nanofiber; polymer nanofibers; ceramic nanofibers

INTRODUCTION

Polymer fibers with nanometer diameters produced by the electrospinning process have attracted more intensive research due to wide potential applications as filtration membranes, catalysts, and in biomedical fields.[1–5] The typical electrospinning process involves the application of a high voltage between an electrically grounded collector and a nozzle supplied with polymer solution (or melt). In the presence of the electric field, the pendent drop is distorted into the shape of a cone. When the electric field at the apex of the cone exceeds a critical strength,[6–14] a continuous jet is ejected which travels to the collection apparatus. At some critical distance from the point of initiation, the jet begins whipping and circling and this is the onset of bending instability stage.[6–14] During this whipping process, the jet is stretched many times its original length to generate continuous fibers with diameters on the nanometer scale. A detailed discussion of recent developments and applications of electrospun fibers can be found in a number of specific application and general review articles.[15–20]

Electrospun fibers are most often collected in the form of a nonwoven textile. This type of fabric architecture is suitable for many of the applications for which electrospun fibers are currently being used. Examples of these applications include tissue engineering,[18] biomedicine,[19] protective garments, and to some extent composite materials fields.[20] Other applications such as composite reinforcement, nanoelectronics, electro-optical, and sensor applications would require oriented or patterned arrays of nanofibers rather than randomly orient mats. However, controlled deposition of electrospun fibers is problematic due to the presence of the bending instability inherent in the process.

Correspondence to: J. M. Deitzel (Jdeitzel@udel.edu).

Contract grant sponsor: Army Research Laboratory-Composite Materials Research Collaborative Program; contract grant number: W911NF-06-2-0011.

A variety of approaches to electrospinning have been investigated to either eliminate or mitigate the effects of bending instability. The simplest approach[21] is to collect the fibers on a rapidly moving target, such as a rotating drum, or combing device. If the surface velocity of the drum is significantly faster than the translational speed of the electrospinning jet, then the consolidated jet is subjected to load in tension that can stabilize the lateral bending instability, if it is not too severe. This approach has been somewhat successful in that fibers collected in this manner are generally oriented in the direction of motion of the target; however, precise alignment of the fibers using this technique is extraordinarily difficult. For polymer–solvent systems that exhibit a vigorous bending instability, like polyethylene oxide (PEO) in water, the electrospinning jet undergoes numerous initiations[7] of bending as it progresses toward a collection target, causing the electrospinning jet to take a VERY complex and meandering path to the collection plate or drum. Eddies in the local electric field and/or air currents further complicate the problem, making collection of HIGHLY oriented fibers very difficult, independent of the rotational speed of the drum.

In 2001, Deitzel et al.[1] used a series of ring electrodes with the same bias as the spinneret to confine the electrospinning jet and effectively eliminated the bending instability, which significantly reduced the area of deposition. More recent work[22] has taken this technique a step further and demonstrated the ability to deposit fibers in specific patterns. The weakness of this approach is that it radically slows the rate of fiber output.[1] Other researchers [2,3,23] have explored various active and passive approaches to control fiber deposition, which have met with varying degrees of success. However, each of these methods has challenges that could limit their usefulness in commercial applications that require high output of fibers. The readers are referred to a detailed review of the different electrospinning approaches by Teo et al.[23]

Theoretical treatment of the electrospinning process[7–9,11,12] suggests that onset and growth of the bending instability occurs as a result of an imbalance in the tangential stress at the air–fluid interface, caused by the interaction of the induced surface charge density at the fluid surface and the external electric field tangent to the fluid surface in the axial direction.[9,11] For a polymer solution with a given viscosity, the stability[8–14] of an electrospinning jet can be characterized as a competition between solution surface tension and surface charge repulsion. If the solution surface tension is the dominant force, then the jet will not deviate from linearity; however, if the repulsive force between surface charges dominates, then a bending instability will initiate and grow. Electrohydrodynamic theory[9] also predicts that small changes in solution viscosity can dramatically limit the initiation and rate of growth of the lateral (bending) instability in electrostatically driven jets. In essence, the viscoelastic response of the polymer solution acts to counter the electrostatic forces, stabilizing the electrospinning jet with respect to this lateral instability. This is consistent with experimental observations[5,13,24] that polymer solutions with high viscosities exhibit much less pronounced bending instability compared with low-viscosity polymer solutions.

Implicit in these works [6–14,25] is the idea that for a given solution viscosity there is a critical density of free charge at the fluid–air interface below which the bending instability will not initiate, or at least be severely dampened by viscoelastic forces and surface tension. In the presence of an electric field, the free charge in an electrospinning solution can originate through chemical reactions with the electrode (referred to as Unipolar injection[25]) or through dissociation of neutral species within the bulk of the solution(i.e., polymer, solvent, and any contaminates that might be present). It is understood[25–27] that the electrostatic energy required to ionize a solute varies approximately with the inverse of the dielectric constant of the solution, therefore dissociation of electrolytic species occurs more readily and completely in solvents with high-dielectric constants, like water and *N*,*N*-dimethyl formamide. Conversely, electrolytic species dissolved in solvents with low-dielectric constants undergo both dissociative and associative chemical reactions at comparable rates, which limit the overall concentration of free charge.[25] In this work, we demonstrate that it is possible to maintain a stable electrospinning jet without the onset of the characteristic bending instability through use of high-purity [high-pressure liquid chromatography (HPLC) grade] solvents with low-dielectric constants. Electrospun fibers produced in this manner can be wound up on a high-speed rotating drum like conventionally produced fibers, while maintaining a high degree of spatial alignment. Furthermore, it will be demonstrated that fiber diameter can be controlled by varying the rate of fiber take up relative to initial velocity of the electrostatically driven jet.

EXPERIMENTAL

Figure 1 shows a schematic of the electrospinning setup used in these experiments. The basic configuration is similar to that described by Hohman et al.,[8] and consists of a stainless steel syringe needle inserted through a metal disc that is positioned above a rotating drum. Unless otherwise specified, fibers were spun at a voltage of $\sim$ 15 kV from a distance of $\sim$ 12 cm from the collection drum. The drum rotational velocities were measured directly using a strobe tachometer. This information was

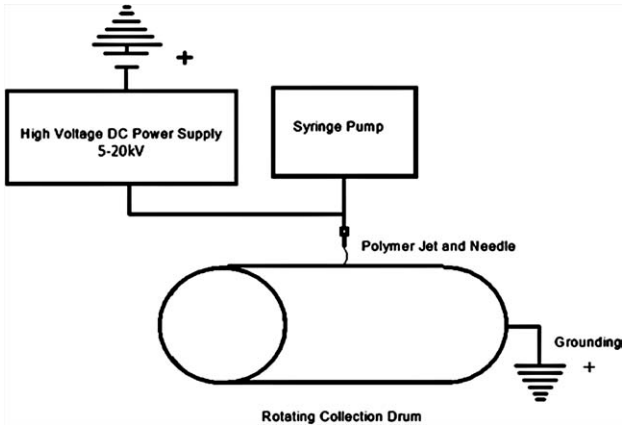

Figure 1 Schematic of the electrospinning setup used for fabricating highly oriented fibers.

used to calculate the drum face velocity. Polymer solution is supplied to the syringe needle using a Harvard Apparatus PHD 2000 syringe pump. In this work, 400,000 PEO has been dissolved in a low-dielectric (HPLC grade chloroform) and high-dielectric (HPLC grade water) solvents in various concentrations. Dielectric constants for both solvents were measured using a custom electrochemical cell consisting of two platinum plates separated by a Delrin spacer. Measurements of dielectric constant as a function of frequency were made over the frequency range of 500 kHz to 10 MHz. The cell constant was determined using an ultrapure water standard ($\varepsilon = 78.54$ at 25°C). The dielectric constant for HPLC grade water was determined to be $\varepsilon = 78.45$ at 25°C, and the dielectric constant for HPLC grade chloroform was determined to be $\varepsilon = 3.85$PEO is well known as a spinnable polymer and is often used as a model system[1,4,5,7,21] for processing studies. The polymer solutions discussed here have been characterized in terms of conductivity, viscosity and surface tension and the results are presented in Table I. Conductivity measurements were made using a VWR Traceable™ Conductivity Meter calibrated with standard 84μs/cm standard solution (HI 7033 from HANNA Instruments). Viscosity measurements were taken on AMVn Automated Micro Viscometer from Anton Paar GmbH with MS 4.0 mm capillary (#11416548). Surface tension was carried out with pendant drop method. Electrospun fibers were characterized with respect to their morphology using a field emission scanning electron microscopy (SEM; JEOL 7400) operated at an accelerating voltage of 3 kV. All samples were coated with gold before imaging. All image analysis was carried out with NIH image software. Wide-angle X-ray diffraction (WAXD) experiments were performed using a Philips Diffractometer PW1821 with Philips 3100 X-ray generator (Cu Ka anode, voltage 30 kV, current 15 mA, and scanning step is 0.02°/step).

RESULTS AND DISCUSSION

Effects of solution properties

The effects of solvent dielectric properties on fiber spatial orientation and morphology can be seen clearly in Figure 2, which shows both optical and electron micrographs of electrospun fibers collected on a rotating drum spinning at 8 m/s. In these images, the direction of the drum rotation is left to right. Figure 2(A,B) shows fibers that have been spun from a 6% solution of 400 K MW PEO dissolved in HPLC grade water (dielectric constant $\varepsilon \sim 78.45$). The breadth of the resulting stripe is approximately 2.5 in. across. In Figure 2(B), the SEM micrograph of fibers removed from a section of the material in Figure 2(A) shows a random orientation of fibers with an average diameter of $\sim$ 200 nm, in spite of the rapid rotation of the collection drum. In Figure 2(C,D), we see fibers that have been spun from 3% PEO dissolved in HPLC grade chloroform (dielectric constant $\varepsilon \sim 4.1$), again collected on the drum spinning at the same rate as the material shown in Figure 2(A,B). Figure 2(C) is an optical micrograph depicting two stripes of fibers that have been collected sequentially in time, by shifting the position of the spinneret by $\sim$ 1 in. [note the scale on the left side of Fig. 2(A,C)]. Examination of the SEM micrographs of samples taken from the stripe in Figure 2(C) shows that these fibers have a very high degree of spatial orientation and diameters ranging from 800 nm to 1.5 μm.

It is important to emphasize that the spinning conditions for each case depicted in Figure 2 are exactly

TABLE I
Electrospinning Solution Properties

Samples	PyFA (mg)	Viscosity (mPa S)	Conductivity (μS/cm)	Surface tension (mN/m)
6% PEO/H_2O	0	1322 ± 0.14	150 ± 2.0	54.8 ± 5.8
3% PEO/$CHCl_3$	0	352 ± 1.30	<0.1	33.6 ± 1.1
3% PEO/$CHCl_3$	142	317 ± 0.60	0.3 ± 0.3	34.2 ± 1.8
3% PEO/$CHCl_3$	208	291 ± 0.39	0.6 ± 0.1	33.7 ± 1.5
3% PEO/$CHCl_3$	384	296 ± 0.15	2.2 ± 0.2	31.5 ± 1.0
3% PEO/$CHCl_3$	843	237 ± 0.50	10.7 ± 0.5	28.9 ± 1.3

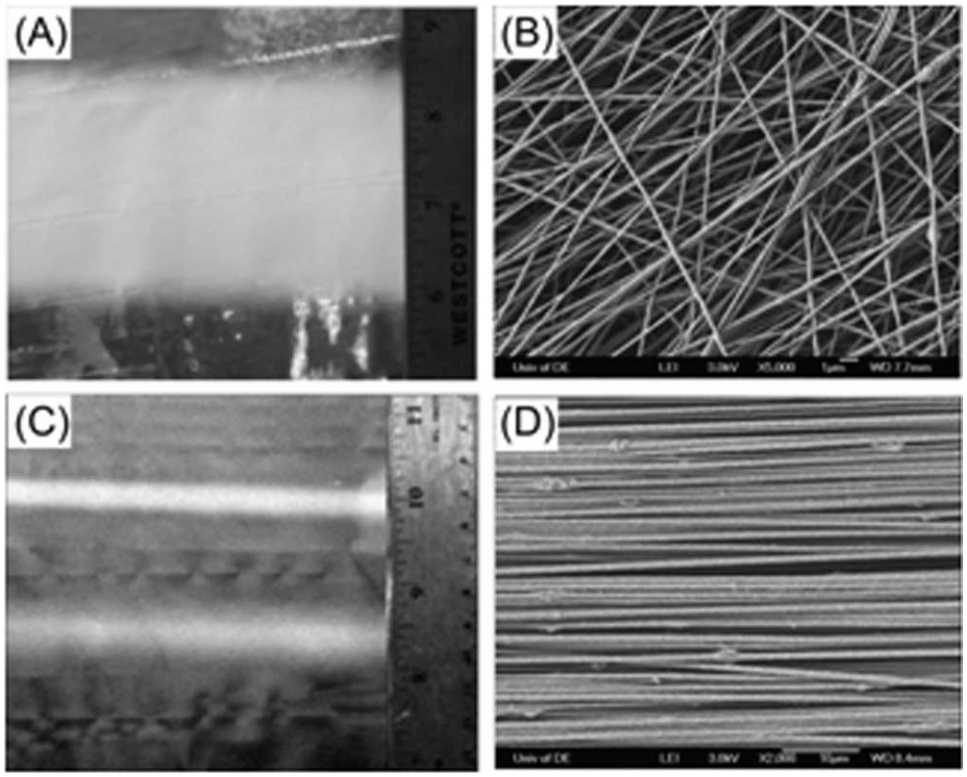

Figure 2 Electrospun PEO collected on a drum for (A) 6% PEO in water, (B) SEM image of sample shown in (A), (C) 3% PEO in chloroform, (D) SEM image of fibers shown in (C). In both cases, spinning distance, 12 cm; spinning voltage, 15 kV; feed rate, 0.3 mL h; and drum speed, 8 m/s.

the same in terms of processing variables (spinning voltage, 15 kV; spinning distance, 12 cm; drum speed, 8m/s; and solution feed rate, 0.3 mL/h). Only polymer concentration and solvent composition are different. As discussed in "Introduction," the random orientation of electrospun fibers in a collected fabric is due to the presence of the lateral bending instability. The high degree of fiber orientation seen in Figure 2(D) suggests that, for fibers spun from the 3% PEO/chloroform solution, the lateral bending instability has either been suppressed mechanically because the drum take-up speed is MUCH faster than the jet speed, or it was never present in the first place.

High speed imaging experiments

To investigate this further, high-speed imaging experiments of the electrospinning process have been carried out to visualize the onset and growth of the lateral instability. For this experiment, the spinning voltage and spinning distances were kept at 15 kV and 12 cm, but the drum was kept motionless (0 m/s) so that the possibility of mechanical stabilization of the jet could be eliminated. This spinning configuration maintains approximately the same electrode geometry used to collect the specimens seen in Figure 2 and eliminates air currents produced by the rotating drum, making imaging of the complete length of the electrospinning jet possible. The images in Figure 3 were collected at different points along the electrospinning jet to determine the point at which the onset of the bending instability occurs.

For the PEO/water systems [Fig. 3(A1,A2)], we see that the onset of the lateral instability occurs $\sim$ 2.3 cm below the tip of the spinning needle, which is consistent with the random orientation of fibers seen in Figure 2(A,B). We observe in the case of the 3% PEO/chloroform Figure 3(B) that the electrospinning jet remains straight all the way to the surface of the rotating drum, with no evidence of the bending instability. This is consistent with the highly aligned fibers seen in Figure 2(D).

From the images in Figure 3(B1,B2), it is clear that the bending instability never initiates for the 3% PEO/chloroform solution and this is why much more narrow stripes of highly oriented fibers are observed in Figure 2(C,D). One possible reason for this is that the 3% solution of PEO/chloroform has a significantly higher viscosity than the 6%PEO/water solution, preventing the initiation of the bending instability, as discussed in "Introduction." However, measurements of the solution viscosities for each case clearly show that the viscosity of the PEO/chloroform solution is much less than that of the PEO water solution (Table I). We hypothesize that the

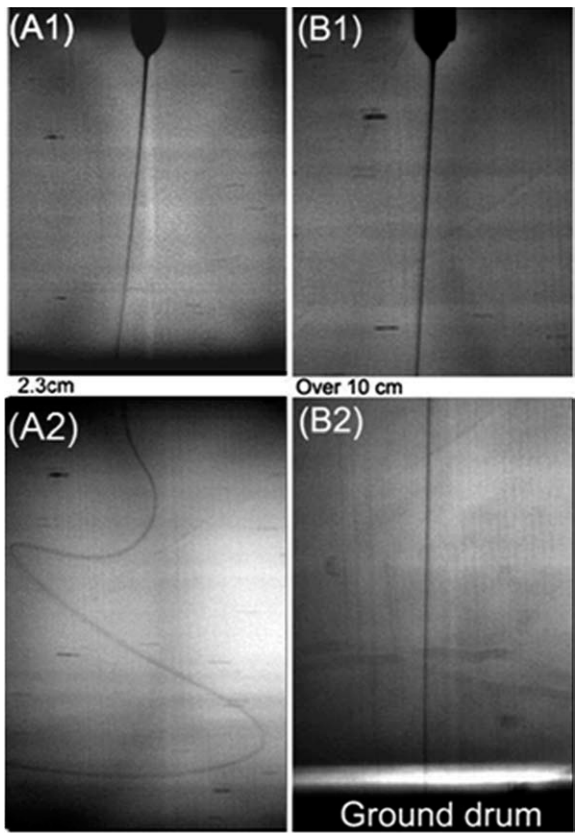

Figure 3 High-speed images of solutions electrospun from (A) 6% PEO in water, (B) 3% PEO in chloroform. Spinning voltage, 15 kV; spinning distance, 12 cm; drum velocity, 0 m/s; and solution feed rate, 0.3mL/h.

low-dielectric constant of the chloroform ($\varepsilon = 3.85$) has limited the available free charge in the solution below the critical value needed to initiate the bending instability.

Dependence of lateral jet stability on solution conductivity

To validate this hypothesis, a series of solutions of 3% PEO/chloroform were made with an increasing amount of an organic salt, to increase the conductivity and the amount ionic species in the polymer solution. Organic ammonium salt,[28,29] as additives, have been shown to effectively increase the conductivity of polymer solutions with little change in surface tension and viscosity. Here, pyridine–formic acid (PyFA, mixture pyridine and formic acid with molar ratio 1/1) was chosen as organic ammonium salt to add into the PEO/$CHCl_3$ solution. From the measured data, it can be seen that the addition of the salt to the PEO/chloroform solution results in some reduction in solution viscosity and has relatively little effect on the solution surface tension (Table I). However, the solution conductivity is increased by three orders of magnitude for the highest salt concentration.

A comparison of SEM micrographs for the fibers collected for each of the PEO/chloroform solutions clearly show that the spatial orientation of the fibers becomes much more random as the solution conductivity increases (Fig. 4), indicating the onset of the lateral bending instability with increasing solution conductivity. Again, for each case depicted in Figure 4, the processing variables are identical and ONLY the salt concentration, and hence the available free charge in the solution, has been varied. Figure 5 shows a plot of fiber diameter as a function of salt content. We see that the average fiber diameter decreases slightly with increasing salt content and the onset of the bending instability. It is worth noting that the uniformity of the fiber diameter decreases significantly as the salt content is increased, as is illustrated by the increase in the coefficient of variation from $\sim 10\%$ to $\sim 50\%$ as a function of salt concentration.

The role of solvent dielectric constant

The physical observation that increasing solution conductivity (i.e., charge density) results in the initiation and growth of nonaxisymmetric perturbations in the electrospinning jet is consistent with discussions in the literature,[7,9] regarding the origin of the bending instability. Initiation and growth of the bending instability are generally attributed to either electrostatic repulsion of free charge on the jet surface[7,9] (Mechanism I) and/or the presence of a dipolar charge distribution induced by lateral fluctuations of the centerline of the jet[7] (Mechanism II). In the first case, the local electrostatic repulsive forces associated with the surface charge must exceed the stabilizing shear force that is tangent to the jet surface[30] In the initial portions of the electrospinning jet (i.e., the cone and initial linear portion of the electrospinning jet), there exists a tangential shear force at the air–fluid interface that results from the interaction of the free charge at the surface with external electric field. As a fluid element in the electrospinning jet travels farther from the point of jet initiation, the magnitude of this tangential shear force, and thus its ability to stabilize the electrospinning jet diminishes.[30] At this point, jet stability is determined by a balance of local electrostatic forces (repulsive), viscous forces, jet inertia, and surface tension. If the surface charge density is large, electrostatic repulsive forces will dominate and any small fluctuation in the jet position relative to the centerline can undergo sustained growth.[7,9]

In the second case, a dipolar charge distribution forms as the charge on the jet surface shifts to accommodate the changes in surface geometry, screening out the electric field inside the jet. The induced dipoles interact with the external electric field, producing a torque that causes the jet to bend

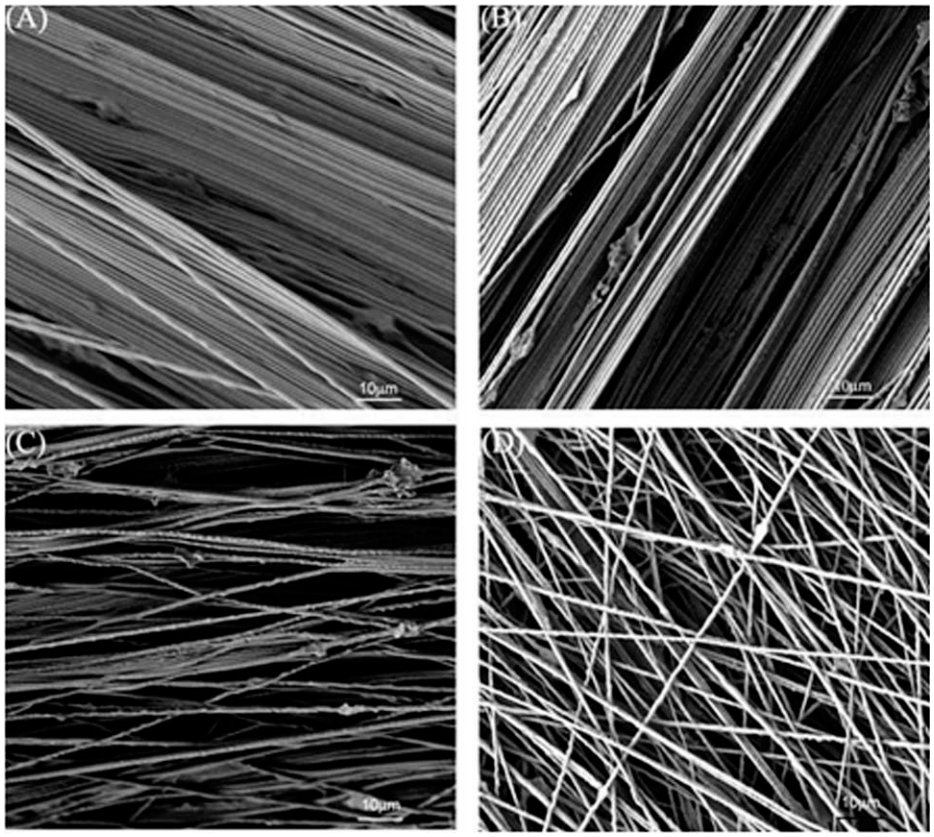

Figure 4 Low magnification SEM images of PEO fibers electrospun from 3 wt % PEO/$CHCl_3$ solution with PyFA (A) 1.37 wt %, $\sigma = 0.3$ μS/cm; (B) 2.09 wt %, $\sigma = 0.6$μS/cm; (C) 3.77 wt %, $\sigma = 2.2$ μS/cm; and (D) 8.43 wt %, $\sigma = 10.7$ μS/cm. Electrospinning at 15 kV, 12 cm, 8.0 m/s, and 0.3 mL/h.

further.[9,31] For this to occur, the characteristic time that it takes for the surface charge move (charge relaxation time, τ) must be small compared with the timescale associated with the mechanical perturbations of the electrospinning jet, so as to be considered "instantaneous."[9,25,32]

The dielectric constant of the solvent plays a critical part for both of the initiation mechanisms described above, by limiting the amount of available free charge for a given concentration of ionic species. As discussed in "Introduction," efficiency of ion disassociation is greatly reduced in solvents with a low-dielectric constant, reducing the amount free charge, which is characterized by a lower solution conductivity (Table I). A reduction in the available charge on the jet surface weakens the electrostatic repulsive force associated with Mechanism I, potentially stabilizing the jet for greater distances from the spinneret.

In addition, the charge relaxation time, τ is simply the ratio of the dielectric constant, ε, and conductivity of the solvent, K.

$$\tau = \varepsilon/K$$

A plot of τ as a function of salt concentration for the PEO/chloroform solutions listed in Table I shows (Fig. 6) that for very low concentrations of ionic species, τ is on the order of ~ 1 μs, which is approaching the exposure time reported by Reneker et al.[7] for visualization of the initiation of the bending instability (<250 μs) for PEO/water systems using high-speed imaging. Equilibration of the distribution of charge on the fluid surface can only be considered

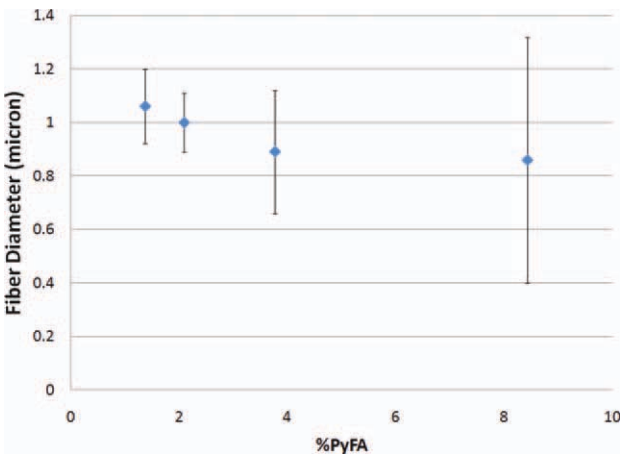

Figure 5 Fiber diameter as a function of PyFA concentration (wt %). [Color figure can be viewed in the online issue, which is available at wileyonlinelibrary.com.]

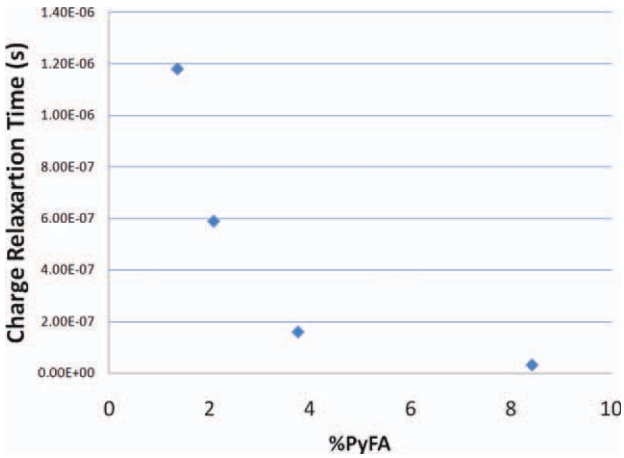

Figure 6 Charge relaxation time as a function of PyFA (wt %). [Color figure can be viewed in the online issue, which is available at wileyonlinelibrary.com.]

"instantaneous," if the charge relaxation time is very small compared with the characteristic time associated with the physical perturbation of the electrospinning jet.[25,32] As a result, the conditions for initiation and growth of the bending instability due to a dipolar distribution of surface charge (Mechanism II) become less favorable as τ increases.

From the discussion above, it is reasonable to expect that there is some critical free charge density (reflected by solution conductivity) at which viscous forces, inertia forces, and surface tension, balance the electrostatic interactions responsible for the bending instability. The result is either complete suppression of the instability or possibly restriction of its manifestation to very long wavelengths, comparable to the distance from the spinneret to collection target. For the PEO/chloroform systems discussed here, that critical conductivity appears to be $\sim$ 0.6 μS/cm). Typically, what is reported in the literature is what Hohman et al.[8,9] refer to as a shift directly from a conductive axisymmetric instability to the bending or "whipping" instability. The likely reason for this is that most polymers of interest are soluble in relatively polar organic solvents, and acids, where ionic species undergo dissociation quite readily. Common solvents used in electrospinning include water, Dimethyl formamide, formic acid, and others.[1–20]

These results have broad implications for processing of submicron fibers using the electrospinning technique and for potential applications in which the fibers may be utilized. By suppressing the bending instability, it is now possible to apply conventional textile processing techniques for control of electrospun fiber properties. In addition, suppression of the bending instability enables collection of highly aligned submicron filaments with relatively uniform diameters in a simple, continuous process that can be utilized in a variety of applications beyond those of traditional textiles, including electronics and sensors. The final two sections of this work demonstrate how traditional fiber take-up can be applied to the electrospinning process, and how this approach for dampening the bending instability can be used produce highly oriented fibers that would be of greater commercial interest than PEO fibers.

Effect of take-up rate on fiber diameter

Given that it is now possible to electrospin fibers without the onset of the lateral bending instability, it should be possible to mechanically draw the fiber by controlling the speed of the collection drum, as long as the face velocity of the collection drum exceeds the velocity of electrospinning jet. To test the feasibility of this approach, fibers were spun from solutions of 3% PEO in chloroform and collected on a rotating drum at different take-up rates. Direct measure of the electrospinning jet velocity for this polymer/solvent system is beyond the scope of this work, however, typical velocities in the linear region of the electrospinning jet have been reported in the literature for PEO/water systems ranging from 0.5 to 1.0 m/s,[12] which is consistent with the results presented in Figure 7(A–E).

Figure 7(A–E) shows SEM micrographs of electrospun fibers that have been collected on a rotating drum at different speeds. In Figure 7(A), the fibers which have been collected at a very slow drum speed of 0.6 m/s. These fibers have been deposited in tight coils characteristic of Euler buckling, indicating that the velocity of the electrospinning jet exceeds the face velocity of the drum. Similar coiled configuration has been reported (deitzel) for PEO fibers spun onto a stationary target using an electrostatic lens to eliminate the bending instability. This means that the fibers have not undergone any mechanical drawing due to the collection process, and the fiber diameter can be considered to be entirely due to electromechanical stretching and solvent evaporation. The fibers in Figure 7(A) exhibit an average fiber diameter of $\sim$ 1618 nm, and for the present discussion are considered the baseline to which the diameter of fibers collected at higher drum velocities are compared. In Figure 7(B–E), the electrospun fibers are clearly oriented in the direction of the drum rotation, indicating that they have been subjected to some degree of mechanical stress due to the collection process.

A plot of average fiber diameter as a function of drum velocity in Figure 8 clearly shows that increasing the rate of fiber uptake leads to significant reduction in fiber diameter, reaching a plateau of $\sim$ 658 nm for velocities of 12 m/s and higher. The average draw ratio resulting from mechanical drawing

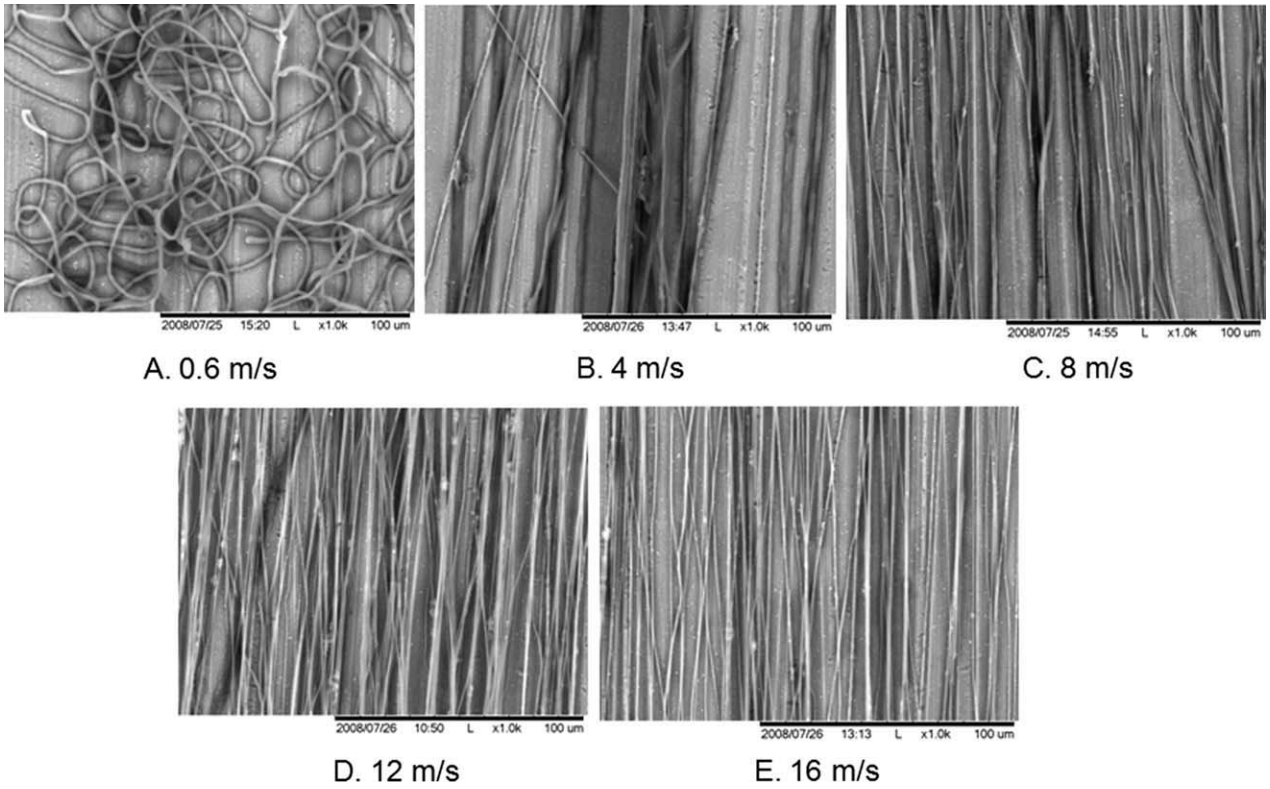

Figure 7 Electrospun fibers PEO fibers collected on a rotating drum for different face velocities (A) 0.6 m/s, (B) 4.0 m/s, (C) 8 m/s, (D) 12 m/s, and (E) 16 m/s.

can be estimated from the ratio of the change in fiber cross section compared with the baseline (Fig. 7A). Based on this, the maximum draw ratio, observed for fibers collected at a drum face velocity of 16 m/s, was $\sim 6\times$. It should be noted that close inspection of fibers collected at a drum speed of 16 m/s (Fig. 9) at high magnification show that the electrospun fibers have undergone localized yielding with a further reduction of fiber diameter to $\sim$ 300 nm, which was not observed for fibers collected at velocities below 12 m/s.

The presence of this necking indicates that the drawing force achieved at high-drum speeds has exceeded the yield strength of the drying filament. The exact conditions under which this yielding occurs is not clear, although it is reasonable to assume that the process is influenced by variables such as the rate of solvent evaporation and

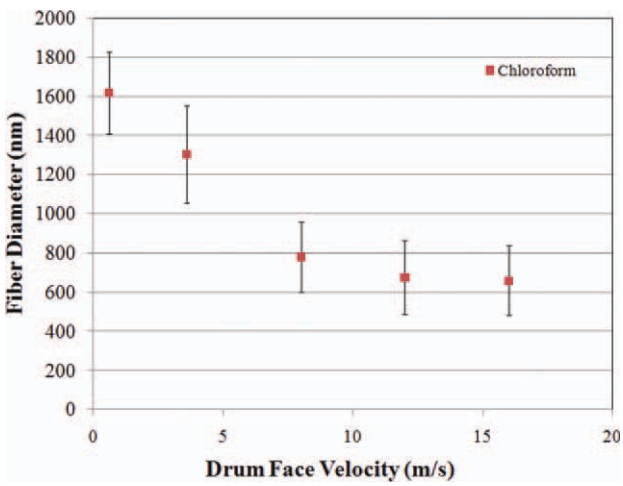

Figure 8 Fiber diameter as a function of take-up drum speed (m/s) for 3% PEO in chloroform. [Color figure can be viewed in the online issue, which is available at wileyonlinelibrary.com.]

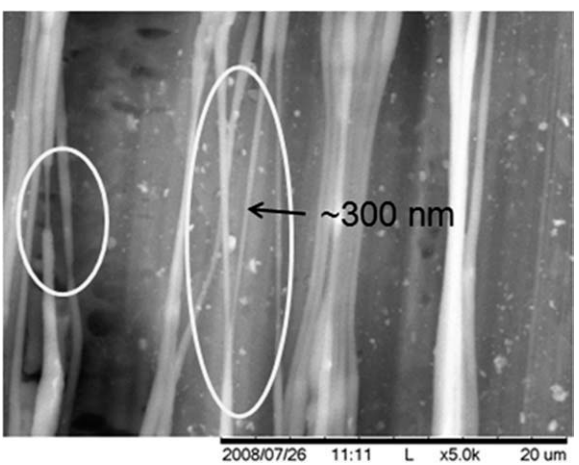

Figure 9 SEM micrograph of oriented electrospun fibers collected on a rotating drum with a face velocity of 16 m/s.

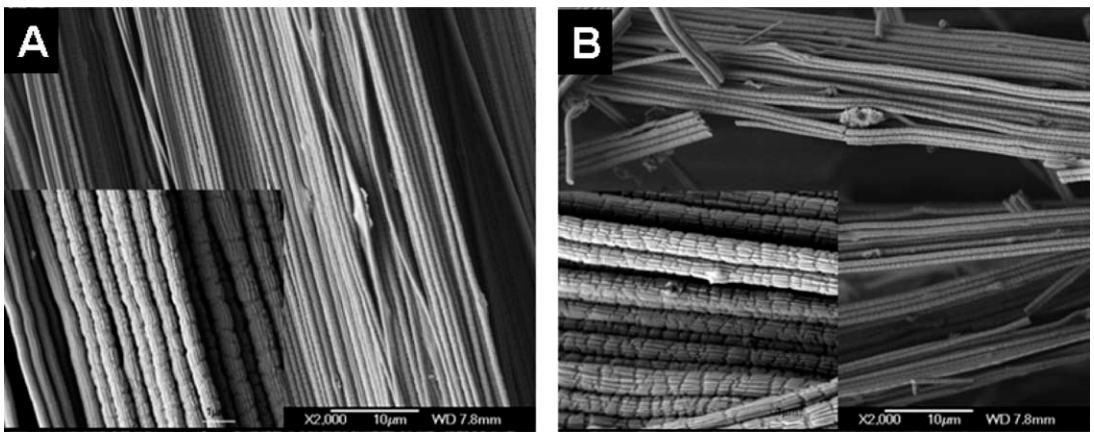

Figure 10 SEM images of highly oriented ceramic fibers made by electrospinning at spinning voltage, 15 kV; spinning distance, 12 cm; solution feed rate, 0.3 mL/h; and drum velocity, 1000 rpm (8 m/s): (A) PEO–TiO_2 fiber; (B) TiO_2 nanocrystals fibers after 500°C for 4 h.

molecular weight of the polymer. Further complicating the issue is the action of air currents on the jet as it progresses toward the rotating drum. During the course of these experiments, it was observed that drum speeds of 12 m/s or greater generated considerable displacement of air in the spinning chamber. This air displacement will significantly affect the rate of solvent evaporation and possibly the draw ratio of the filament as the material is collected on the drum. At this point, it should be pointed out that the process described here should not be considered "optimized." It should be possible to draw the electrospun fiber down to a diameter of 200–300 nm by controlling the rate of evaporation through either the temperature and/or composition of the ambient atmosphere and eliminating, or mitigating these air currents.

Inorganic fibers

In addition to pure polymers, ceramic, metal, and metal oxide precursors can be introduced into the polymer solution and spun. The resulting fibers can then be calcinated to produce pure ceramic, metal, and metal oxide fibers with submicron diameters. Fibers of this type would be of interest for a wide variety of electronic and sensor applications, especially in the form of highly aligned networks. However, most of the precursors for these class of materials are ionic in nature and may potentially raise the free charge content of a low-dielectric solution past the critical conductivity that initiates the onset of the lateral bending instability, inhibiting the ability to produce highly oriented fibers.

To explore the possibility of obtaining oriented inorganic fibers, a polymer solution of PEO and chloroform containing a metal alkoxide was electrospun[33] in an attempt to form orientated metal oxide fibers. Amorphous oxide fibers were obtained by rapid hydrolysis in the air and then transform them into nanocrystal oxide fibers by calcination at high temperature, removing the last of the organic material. Figure 10(A) shows the electrospun PEO–TiO_2 fibers obtained by mixing 0.5 g of $Ti(O^iPr)_4$ into 10 mL 3 wt % PEO/$CHCl_3$ solution. The fiber has some nanometer scale stripes with about 80 nm width along the fiber due to the phase separation. The $Ti(O^iPr)_4$ will rapidly hydrolyze and condense to form TiO_2 in air because acid is added as retarding agent. Cracks are observed on the PEO–TiO_2 fibers' surface which may arise from the stretching of the fiber that occurs as it is collected on the rotating drum.

Figure 10(B) shows the TiO_2 fiber produced from $Ti(O^iPr)_4$–PEO fiber calcinated at 500°C over 4 h. The average diameter of the TiO_2 fibers after calcination is 650 nm. WAXD experiments were carried out for the TiO_2 after calcination at 500°C. An example of the WAXD pattern is shown in Figure 11. The diffraction peaks at $2\theta = 25.5$, 37.5, 47.8, 54, 55.2, and

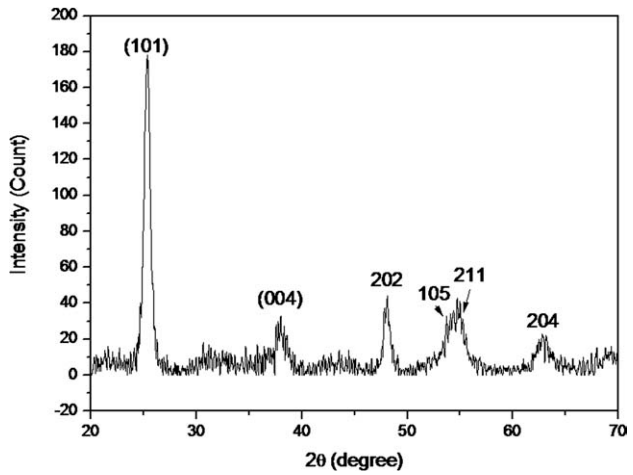

Figure 11 XRD pattern of TiO_2 anatase nanocrystal fiber calcinated at 500°C for 5 h.

62.5 were ascribed to the (101), (004), (200), (105), (211), and (204) peaks of the anatase crystal modification of TiO_2, respectively. The average crystal size in the calcinated fibers was estimated to be about 12.6 nm using the Debye–Scherrer formula:

$$D_{hkl} = k\lambda/\beta\cos\theta,$$

where $k = 0.9$; λ, wavelength of the radiation, $\lambda_{Cu} = 1.54056$ Å; β, full width at half maximum in radian; and θ, the incident scattering angle.

These results show that this method could be further extended to fabricate the highly oriented nanocrystal "wires" for a wide variety of conductive, semiconductive, and superconductive materials.

CONCLUSIONS

A simple approach to electrospinning has been developed that for the first time enables the collection of continuous polymer, ceramic, and multiphase composite fibers, in quantity, with a high degree of spatial orientation. It has been demonstrated experimentally that it is possible to prevent initiation of the lateral "bending" instability inherent in the electrospinning process by use of solvents with low-dielectric constants and high purity, which limit the amount of "free" charge that can be induced in the polymer solution during spinning. The results presented here are qualitatively consistent with theoretical predictions published in the literature and suggest that for a given polymer/solvent system there is critical concentration of "free" charge, below which the lateral bending instability will not initiate. This enables the electrospun fibers to be wound up on a rotating drum in a conventional manner, providing a way to collect highly oriented electrospun fibers in large quantities. Draw ratio's as high as 6× were achieved experimentally for PEO/chloroform solutions. This work also illustrates the role that ionic and ionizable species present in polymer solutions play in the initiation of the lateral bending instability of the electrospinning jet. These results have important implications for the scaled-up production of nanofiber fabrics containing charge carrying species, such as ionic biocidal agents, metallic salts, carbon nanotubes, and ceramic precursors and emphasize the critical need for a greater understanding of the electrochemical processes that are at work during electrospinning.

The authors thank Dr. Serge Lopatnikov and Dr. Mathew Helgeson for helpful discussions concerning fundamental nature of electrostatically driven jets. We would also like to thank Mr. Peter Beltramo for kindly for his help determining the dielectric constants for solvents used in this work.

References

1. Deitzel, J. M.; Kleinmeyer, J. D.; Hirvonen, J. K.; Tan, N. C. B. Polymer 2001, 42, 8163.
2. Zussman, E.; Theron, A.; Yarin, A. L. Appl Phys Lett 2003, 82, 973.
3. Li, D.; Wang, Y. L.; Xia, Y. N. Nano Lett 2003, 3, 1167.
4. Fong, H.; Chun, I.; Reneker, D. H. Polymer 1999, 40, 4585.
5. Deitzel, J. M.; Kleinmeyer, J.; Harris, D.; Tan, N. C. B. Polymer 2001, 42, 261.
6. Yarin, A. L.; Koombhongse, S.; Reneker, D. H. J Appl Phys 2001, 90, 4836.
7. Reneker. D. H.; Yarin, A. L.; Fong, H.; Koombhongse, S. J Appl Phys 2000, 87, 4531.
8. Hohman, M. M.; Shin, M.; Rutledge, G.; Brenner, M. P. Phys Fluids 2001, 13, 2221.
9. Hohman, M. M.; Shin, M.; Rutledge, G.; Brenner, M. P. Phys Fluids 2001, 13, 2201.
10. Thompson, C. J.; Chase, G. G.; Yarin, AL.; Reneker, D. H. Polymer 2007, 48, 6913.
11. Feng, J. J. Phys Fluids 2002, 14, 3912.
12. Helgeson, M. E.; Grammatikos, K. N.; Deitzel, J. M; Wagner, N. J. Polymer 2008, 49, 2924.
13. Rutledge, G. C.; Fridrikh S. V. Adv Drug Del Rev 2007, 59, 1384.
14. Theron, S. A.; Zussman, E.; Yarin, A. L. Polymer 2004, 45, 2017.
15. Dzenis, Y. Science 2004, 304, 1917.
16. Li, D.; Wang, Y. L.; Xia, Y. N. Adv Mater 2004, 16, 361.
17. Park, S.; Park, K.; Yoon, H.; Son, J.; Min, T.; Kim, G. Polym Int 2007, 56, 1361.
18. Smith, L. A.; Ma, P. X. Colloids Surf B Biointerfaces 2004, 39, 125.
19. Burger, C.; Hsiao, B. S.; Hsiao, C.B. Annu Rev Mater Res 2006, 36, 333.
20. Jayaraman, K.; Kotaki, M.; Zhang, Y. Z.; Mo, X. M.; Ramakrishna, S. J Nanosci Nanotechnol 2004, 4, 52.
21. Doshi, J.; Reneker, D. H. J Electrostatics 1995, 35, 151.
22. Bellan, L. M.; Craighead, H. G. J Vacuum Sci Technol B 2006, 24, 3179.
23. Teo, W. E.; Ramakrishna, S. Nanotechnology 2006, 17, R89.
24. Baumgart, Pk. J Colloid Interface Sci 1971, 36, 71.
25. Saville, D. A.; Annu Rev Fluid Mech 1997, 29, 27.
26. Baygents, J. C.; Saville, D. A. J Colloid Interface Sci 1991, 146, 9.
27. Kumar, R.; Sharma, J. P.; Sharma, Sekon, S. S. Eur Polym J 2005, 41, 2718.
28. Hou, H. Q.; Jun, Z.; Reuning, A.; Schaper, A.; Wendorff, J. H.; Greiner, A. Macromolecules 2002, 35, 2429.
29. Huang, C. B.; Chen, S. L.; Lai, C. L.; Reneker, D. H.; Qiu, H, Ye, Y.; Hou, H. Q. Nanotechnology 2006, 17, 1558.
30. Hayati, I. Colloids Surf 1992, 65, 77.
31. Shin, Y. M.; Hohman, M. M.; Brenner, M. P.; Rutledge, G. C. Appl Phys Lett 2001, 78, 1149.
32. Ganan-Calvo, A. M. J Fluid Mech 1997, 335, 165.
33. Bognitzki, M.; Czado, W.; Frese, T.; Schaper, A.; Hellwig, M.; Steinheart, M.; Greiner, A.; Wendorff, J. H. Adv Mater 2001, 13, 70.